# T1a renal cell carcinoma on unenhanced CT: analysis of detectability and imaging features

**Aiko Gobara[1]** (ID)**, Takeshi Yoshizako[1]** (ID)**, Rika Yoshida[1]** (ID)**,
Megumi Nakamura[1]** (ID)**, Hiroaki Shiina[2] and Hajime Kitagaki[1]**

## Abstract

**Background:** Increasing use of unenhanced computed tomography (CT) has been associated with the increasing incidental detection of renal cell carcinoma (RCC) at an earlier stage.
**Purpose:** To evaluate the characteristics in detecting and differentiating T1a RCCs on unenhanced CT.
**Material and Methods:** We retrospectively reviewed 68 patients with 68 T1a RCCs and 39 benign regions. Two radiologists interpreted the images on unenhanced axial CT and performed a blinded and independent review of T1a RCCs. The readers evaluated the presence of RCC and differentiated the detected lesions.
**Results:** The consensus of two readers detected 53 (78%) RCCs. Of the 53 detected RCCs, 42 (62%) RCCs were correctly diagnosed and 11 (16%) masses were misdiagnosed as benign. Of the 39 benign regions, 29 (74%) cysts were diagnosed correctly, but 10 (26%) cysts were misdiagnosed as malignant. The following values of the radiologists were obtained by consensus: sensitivity = 61.8% (42/68); specificity = 74.4% (29/39); positive predictive value = 80.8% (42/52); negative predictive value = 55.0% (29/55); accuracy = 66.4% (71/107). The receiver operating characteristic curve of consensus was 0.754. Inter-observer correlation was $\kappa = 0.849$. There was a significant difference in tumor size ($P = 0.019$) and the contour type of tumor ($P = 0.0207$) between correctly diagnosed RCCs and not correctly diagnosed RCCs.
**Conclusion:** Our findings showed that tumor size and contour type could affect the detection and differentiation of T1a RCC on unenhanced CT. To detect and differentiate T1a RCC on unenhanced CT is difficult. However, the findings from this study may help detection of RCCs on unenhanced CT.

## Introduction

Unenhanced computed tomography (CT) has an important role in the detecting and monitoring of masses, screening for cancer, and evaluation of various conditions in patients for whom the use of intravenous contrast medium is contraindicated (1). Unenhanced CT is a helpful diagnostic examination for acute flank pain due to the high inter-observer agreement, good accessibility, rapid imaging, and non-requirement for intravenous contrast administration (2,3).

The increasing use of CT, especially the increase of contrast-enhanced CT has been associated with an increase in the incidental detection of renal cell carcinoma (RCC), with a shift toward finding smaller tumors at an earlier stage (4–6). Past studies have demonstrated that incidentally detected RCCs are likely to be smaller than symptomatic RCCs, which increases

[1]Department of Radiology, Shimane University Faculty of Medicine, Izumo, Japan
[2]Department of Urology, Shimane University Faculty of Medicine, Izumo, Japan

**Corresponding author:**
Aiko Gobara, Department of Radiology, Shimane University Faculty of Medicine, P.O. Box 00693-8501, 89-1 Enyacho, Izumo, Japan.
Email: aikogobara@gmail.com

to 60–70% of masses <4 cm (7–9). Under such circumstances, it is important to analyze and understand the detectability and characteristic imaging features of small RCCs on unenhanced CT screening. On unenhanced CT, a small and early stage RCC is difficult to detect because of the morphological characteristics of these tumors and lack of the characteristic tumor enhancement pattern on contrast-enhanced CT. In renal masses, the classic definition of "small" is ≤3–4 cm (10–12). This study focuses on the challenging situation of small renal lesions; here, "small" refers to a lesion <4 cm which corresponds to the latest TNM category T1a (13).

RCCs were a rare (in the 1% range) finding at unenhanced CT and differentiating them from benign cyst on unenhanced CT is difficult in many cases (14). Previous studies have evaluated the characteristic image findings of RCC on unenhanced CT (15–18); however, over one-third (37%) of potentially detectable cancers were missed or incorrectly interpreted on unenhanced CT (14). Moreover, these studies were not focused on only T1a RCC, which could be done minimally invasive treatment.

Therefore, the purpose of this retrospective study is to evaluate the role of an abdominal screening unenhanced CT in the detection and differentiation of T1a RCCs from benign lesions.

## Material and Methods

### Study population

Both Institutional Review Board approval and informed consent were obtained for this retrospective study. Electronic medical records from our institution were searched to identify patients who underwent preoperative CT and subsequent partial or radical nephrectomy for RCC from September 2011 to August 2016. Among the 70 patients confirmed to have T1a RCC upon reviews of surgical and pathologic records, two patients with autosomal dominant polycystic kidney disease (ADPKD) were excluded, due to difficulties in the detection of small RCCs. The other 68 patients (47 men, 21 women; age range = 28–84 years; mean age = 65.1 years) were included in this study. None of them had multiple RCCs or previous surgery for urologic malignancy. All patients had undergone both unenhanced and contrast-enhanced CT.

The individuals had a total of 68 T1a RCCs and 39 benign lesions (37 cysts and two columns of Bertin); no other benign lesions (e.g. angiomyolipomas, oncocytoma) were included. The gold standard for diagnosis was histopathology of RCCs and contrast-enhanced CT to obtain evidence for being benign cysts. Unenhanced and contrast-enhanced CT examinations were
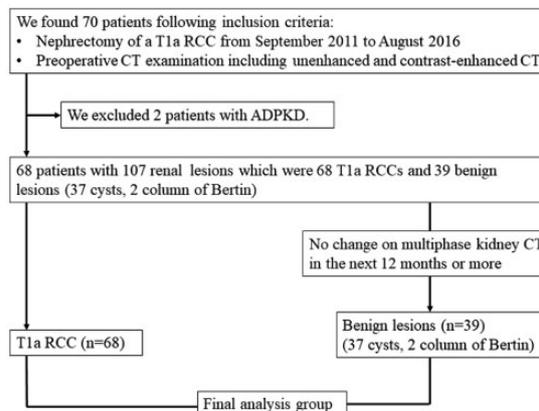


**Fig. 1.** A flowchart of patient selection.

performed as a multiphase examination before surgery. CT protocol consisted of acquisition of an unenhanced CT image (slice thickness = 5 mm) of the kidneys, followed by a corticomedullary phase, delayed nephrographic phase, and excretory phase acquisition. None of the benign lesions co-existing with RCC had histopathological evidence, but they showed no change on multiphase contrast-enhanced CT after 12 months or longer. Fig. 1 displays a flowchart of patient selection.

### CT technique

Unenhanced CT scans of the abdomen were obtained with a 320 multidetector-row CT (Aquilion ONE, Toshiba Medical Systems, Tokyo, Japan). Our standard CT renal scanning protocol was as follows: tube voltage = 120 kVp; tube current = 170–560 mA (depending on patient size); slice thickness = 0.5 mm; reconstructed slice thickness = 5.0 mm; pitch = 0.938; and matrix = $512 \times 512$. The reconstructed slice thickness was 5.0 mm because it was considered to be the standard thickness for abdominal screening.

### Image analysis

Using a picture archiving and communication system (PACS) workstation, two radiologists (with 16 years and four years of experience, respectively) interpreted the CT images and performed a blinded and independent review of the unenhanced CT images of each tumor. The readers were blinded to the location and side of the RCC. Only axial images were evaluated with varying window settings being used to highlight the characteristic findings of RCC. This approach is assumed to be an opportunity to screen the abdomen on unenhanced CT. Each radiologist assessed tumor attenuation (hyperdense, isodense, or hypodense compared to normal renal parenchyma) and categorized the tumors as either homogeneous or heterogeneous

based on subjective visual inspection (15). Tumors were also categorized into the following three groups by the results of pathologic examination: exophytic (>50% of the tumor projected outside the renal cortex); mesophytic (<50% of the tumor projected outside the renal cortex); and endophytic (the tumor was entirely surrounded by uninvolved renal parenchyma). Furthermore, the tumor location was defined by determining the location score: 1 = tumor above or below polar lines (polar lines are defined by the renal vascular pedicle); 2 = tumor crossing polar lines by <50%; and 3 = tumor crossing polar lines by >50%, or tumor between polar lines, or tumor crossing the axial midline (19).

The readers evaluated the presence of RCC and differentiated the detected lesion respectively. First, the kidneys of each patient were specifically evaluated for the possible presence of RCC. Diagnostic criteria for detecting a renal focal mass were defined as: a lesion protruding from the renal parenchyma; and/or a lesion with heterogeneous attenuation; and/or with higher or lower attenuation compared to the renal parenchyma. The senior radiologist measured the maximal diameter of the tumors in any single axial plane on enhanced CT. Each detected lesion was also assessed to determine whether it was benign. The imaging criteria for differentiating RCCs were a lesion with characteristics suggesting possible malignancy (heterogeneous attenuation, homogeneous attenuation not showing water attenuation, unclear margin, thick calcification, and/or septae) and without fat attenuation. Each detected lesion was categorized into two groups: not benign (possibly RCC) or benign. The radiologists known that each participant had at least one RCC and were not allowed to review contrast-enhanced CT images during this session. The contrast-enhanced CT were reviewed as the gold standard for diagnosis after all the evaluations.

The diagnostic capability of each reader for T1a RCC and the results achieved by consensus were determined by calculating the sensitivity, specificity, positive predictive value (PPV), negative predictive value (NPV), accuracy, and area under the receiver operating characteristic (ROC) curve (AUC) for RCC. When the readers disagreed about the diagnosis, the consensus of two readers was used for statistical analysis. To assess inter-observer variability, the kappa statistic was calculated. A kappa value ≤0.20 was considered to indicate slight agreement, 0.21–0.40 was fair agreement, 0.41–0.60 was moderate agreement, 0.61–0.80 was substantial agreement, and ≥0.81 was almost perfect agreement (20).

## Statistical analysis

The Kolmogorov–Smirnov test was used to determine whether the lesion size showed a normal distribution for the RCCs and the benign lesions. The imaging features (size, location, attenuation, contour, and internal characteristics) of detectable RCCs, undetectable RCCs, correctly diagnosed RCCs, incorrectly diagnosed RCCs, and detectable and misdiagnosed RCCs were compared using the Welch t-test for numerical values and the Kruskal–Wallis test as appropriate.

Statistical analysis was performed by using the Statistical Package for the Social Sciences (SPSS), version 23.0 for Windows (IBM Corp., Armonk, NY, USA). $P < 0.05$ was considered a significant difference.

## Results

The characteristics of patients with T1a RCC and the features of renal lesions are provided in Table 1. Benign lesions had a wide range of size, because patients were selected by the existence of T1a RCC. Of the 68 patients, 16 patients had two or more benign cysts: one patient had four benign cysts; three patients had three benign cysts; and 12 patients had two benign cysts. Two of the benign lesions were diagnosed as columns of Bertin from the findings on subsequent contrast-enhanced CT. Of the 37 benign cysts, 35 cysts were water attenuation and two cysts were high attenuation (>20 HU).

The overall AUC, sensitivity, specificity, PPV, and NPV of both readers and their consensus findings for detection of RCC on unenhanced CT are shown in Table 2. The inter-observer correlation was very high with almost perfect agreement according to kappa statistics ($\kappa = 0.849$).

A summary of the results obtained by consensus is shown in Table 3. By consensus, the two radiologists detected 53 RCCs (78%) and undetected 15 RCCs (22%). Of the RCCs detected, 42 tumors (62%) were

**Table 1.** Characteristics of patients and renal lesions.

| Characteristic | Finding |
|---|---|
| Patients | 68 |
| M:F | 47:21 |
| Age (years), mean (range) | 65.1 (38–84) |
| Renal cell carcinoma (n) | 68 |
| Size (mm), mean (range) | 26 (10–40) |
| Clear cell type | 55 (80.9) |
| Papillary type | 8 (11.8) |
| Chromophobe type | 3 (4.4) |
| Other type | 2 (2.9) |
| Benign lesions (n) | 39 |
| Size (mm), mean (range) | 33 (8–70) |
| Cyst | 37 (94.9) |
| Column of Bertin | 2 (5.1) |
| Total lesions | 107 |

Data are presented as n (%) unless otherwise specified.

**Table 2.** Diagnostic capability of T1a RCC.

|  | Sensitivity | Specificity | PPV | NPV | Accuracy | AUC |
|---|---|---|---|---|---|---|
| Reader 1 | 48/68 (70.5) | 31/39 (79.5) | 48/56 (85.7) | 31/51 (60.8) | 79/107 (73.8) | 0.75 |
| Reader 2 | 41/68 (60.3) | 35/39 (89.7) | 41/45 (91.1) | 35/62 (56.5) | 76/107 (71.0) | 0.75 |
| Consensus | 42/68 (61.8) | 29/39 (74.4) | 42/52 (80.8) | 29/55 (55.0) | 71/107 (66.4) | 0.754 |

The figures in parentheses indicate percentage unless otherwise indicated.
PPV, positive predictive value; NPV, negative predictive value; AUC, area under receiver operating characteristic curve.

**Table 3.** Summary of imaging diagnosis.

|  | Renal cell carcinoma | Benign lesion |
|---|---|---|
| Detected and correctly diagnosed | 42 (62) | 29 (74) |
| Detected and incorrectly diagnosed | 11 (16) | 10 (26) |
| Undetected | 15 (22) | 0 (0) |
| Total | 68 (100) | 39 (100) |

Data are presented as n (%).

correctly diagnosed as not benign and 11 tumors (16%) were misdiagnosed as benign. On the other hand, 29/39 benign lesions (74%) were correctly diagnosed and 10/39 benign lesions (26%) were misdiagnosed as not benign. Of the undetected 15 RCCs, 12 were clear cell type, two were chromophobe type, and one was a mucinous tubular and spindle cell carcinoma. Of the 11 detected and incorrectly diagnosed RCCs, 10 were clear cell type and one was papillary type.

The anatomical and imaging characteristics of detectable RCCs, undetectable RCCs, correctly diagnosed RCCs, incorrectly diagnosed RCCs, and detectable and misdiagnosed RCCs are displayed in Table 4. The correctly diagnosed RCCs were larger than the incorrectly diagnosed RCCs ($27 \pm 8.4$ mm vs. $23 \pm 9.2$ mm). There was a significant difference in size between correctly diagnosed RCCs and incorrectly diagnosed RCCs ($P = 0.019$). In addition, there was a significant difference of tumor contour between undetectable RCCs and detectable RCCs ($P = 0.0003$). Detectability improved as tumor projection from the renal cortex became more prominent. Moreover, there was a significant difference of tumor contour between correctly diagnosed RCCs and incorrectly diagnosed RCCs ($P = 0.0207$). Differentiation also improved as tumor projection from the renal cortex became more prominent. A representative case is shown in Fig. 2.

## Discussion

The present study revealed that the sensitivity of consensus diagnosis for detection of T1a RCC on unenhanced CT was 61.8% with a high inter-observer correlation ($\kappa = 0.849$). There was a significant difference of tumor size ($P = 0.019$) and tumor contour

($P = 0.0207$) between correctly diagnosed RCCs and incorrectly diagnosed RCCs.

As unenhanced CT has become increasingly frequent, there have been more reports about the detectability of RCC by this CT modality. Jung et al. reported an AUC of small (<3 cm) RCC (0.70–0.78), which was significantly lower than that of large RCC (0.97–0.99, $P < 0.001$) (16). Similarly, our study indicated that it is challenging to detect T1a RCC on unenhanced CT because the AUC for consensus diagnosis was 0.754. Sahi et al. reported that unenhanced CT showed good performance for the detection of T1a RCC, with an overall AUC of 0.879–0.923, which may be due to the use of multiplanar reformations (21). Our study demonstrated that the detection and differentiation of T1a RCC is difficult even when the existence of cancer is known.

In the present study, the correct diagnosis rate of T1a RCC on unenhanced CT improved as the tumors became larger and as the tumors showed more projection from the renal cortex. These results suggest that identification of T1a RCC on unenhanced CT is greatly influenced by the pattern of tumor growth. In previous studies, tumor size and tumor contour have been found to influence the detection of RCC on unenhanced CT (16) and our study yielded similar findings. While most large or exophytic RCCs can be detected easily, detection of small and endophytic tumors is problematic. Protrusion from the renal parenchyma enables reviewers to visually and easily recognize small RCC as a mass. In addition, our study suggested the imaging characteristics of the tumor and its location sometimes influence the detectability of T1a RCC on unenhanced CT, although the differences were not statistically significant. In the present study, 15 RCCs were not to get detected even when the readers knew that the patient has at least one focal mass. Twelve RCCs of undetected 15 RCCs located in the upper or inferior pole of the kidney. It was difficult to detect T1a RCCs located in the upper or inferior pole of the kidney and/or tumors showing iso-density compared to the renal parenchyma by only viewing unenhanced axial CT images. When considering the difference between correctly diagnosed RCCs and detectable and misdiagnosed RCCs, the result implies homogeneity of detectable and

**Table 4.** Analysis of imaging features of T1a RCC (n = 68).

| Imaging features | Detectable RCCs (n = 53) | Undetectable RCCs (n = 15) | Correctly diagnosed RCCs (n = 42) | Incorrectly diagnosed RCCs (n = 26) | Detectable and misdiagnosed RCC (n = 11) |
|---|---|---|---|---|---|
| Size (mm), mean ± SD | 26 ± 8.4 | 21 ± 5.4 | 27 ± 8.4[#] | 23 ± 9.2[#] | 23 ± 9.7 |
| Location score* | | | | | |
| 1 | 28 (52.8) | 12 (80) | 22 (52.4) | 18 (69.2) | 6 (55) |
| 2 | 9 (17.0) | 1 (7) | 9 (21.4) | 1 (3.8) | 0 (0) |
| 3 | 16 (30.2) | 2 (13) | 11 (26.2) | 7 (27.0) | 5 (45) |
| Attenuation | | | | | |
| High | 3 (5.7) | 0 (0) | 2 (5) | 1 (3.8) | 1 (9) |
| Iso | 23 (43.4) | 10 (67) | 19 (45) | 14 (53.8) | 4 (36) |
| Low | 27 (50.9) | 5 (33) | 21 (50) | 11 (42.4) | 6 (55) |
| Contour type[†] | ## | ## | ### | ### | |
| Exophytic | 27 (50.9) | 1 (6.7) | 22 (52.4) | 6 (23.1) | 5 (45) |
| Mesophytic | 25 (47.2) | 10 (66.7) | 19 (45.2) | 16 (61.5) | 6 (55) |
| Endophytic | 1 (1.9) | 4 (26.6) | 1 (2.4) | 4 (15.4) | 0 (0) |
| Internal property | | | | | |
| Homogeneous | 18 (34.0) | 6 (40) | 12 (29) | 12 (46.2) | 6 (55) |
| Heterogeneous | 35 (66.0) | 9 (60) | 30 (71) | 14 (53.8) | 5 (45) |

Data in parentheses indicate percentage unless otherwise indicated.

*The location of tumor was defined using location score: 1 = lesions above or below polar lines (polar lines are defined by the renal vascular pedicle); 2 = lesions cross polar lines <50%; 3 = lesions cross polar lines >50% or between polar lines or crossing axial midline (19).

[†]Tumors were also categorized into three groups by contour type of the tumor in the pathologic examinations: lesions that projected >50% outside the renal cortex were defined as "exophytic"; those that projected <50% as "mesophytic"; and those that were entirely encircled by uninvolved renal parenchyma as "endophytic."

The Detectable RCCs group (n = 53) consists of the Correctly diagnosed group (n = 42) and Detectable and misdiagnosed group (n = 11).

The Incorrectly diagnosed RCCs group (n = 26) is the Undetectable RCCs group (n = 15) and the Detectable and misdiagnosed group (n = 11).

Welch t-test for numeric values and Kruskal–Wallis test statistic were used: [#] = 0.019; [##] = 0.0003; [###] = 0.0207.
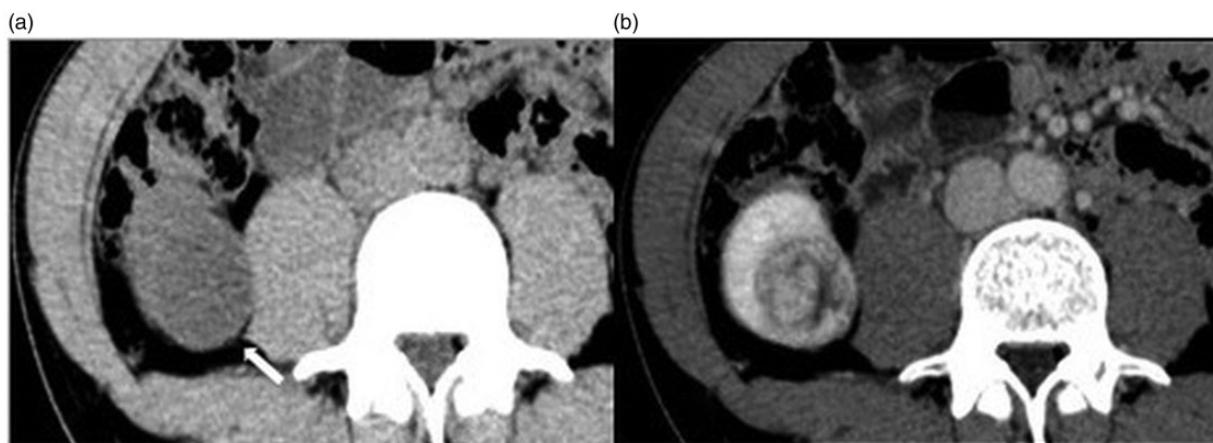


**Fig. 2.** A 38-year-old man with clear cell RCC. (a) Unenhanced image; (b) contrast-enhanced image. On axial unenhanced CT, a 3.5-cm homogeneous low-density mass measuring 20 HU with a clear margin is detected in the right kidney (Rt. Kidney, arrow). The mass projects outside the renal cortex. It is easily detected, but apparently looks like a complicated cyst. On axial contrast-enhanced CT, the mass is heterogeneously enhanced. Therefore, this mass is suggested to be malignant tumor, such as RCC.

misdiagnosed RCCs (55%) may have caused the misdiagnosis. Multiplanar reconstructions could help to overcome this problem and it is currently a standard of care. If a small RCC is homogenous and iso-intense relative to the renal parenchyma, we need special image display techniques to identify it on unenhanced CT. The value of a "liver window" (width = 150 HU; level = 88 HU) setting for detecting small RCCs on unenhanced CT scans has been reported (21). When examining renal lesions, it is important to be aware

of these imaging characteristics of T1a RCCs on unenhanced CT and the limitations of unenhanced CT scans for making a diagnosis.

Our results suggested that the internal characteristics of renal masses had limited usefulness for differentiating T1a RCCs although the differences were not statistically significant. In previous studies, the density of most RCCs has been in the range of 20–70 HU (15). However, a few solid RCCs can show similar attenuation to water (-10–20 HU) on unenhanced CT (18). In our study, none of the RCCs showed water attenuation. However, of 11 detectable and misdiagnosed RCCs, 10 RCCs showed low or iso-attenuation compared to the renal parenchyma and the ROI attenuation of their RCCs was in the range of 20–70 HU. When a heterogeneous renal lesion is found on unenhanced CT, it will probably be diagnosed as a malignancy, even if it has similar attenuation to water. Heterogeneity is crucial to the CT evaluation of renal masses and it is a major determinant of when to get a renal protocol CT for managing an incidental renal mass on unenhanced CT (22). When unenhanced CT is available, a non-fat-containing renal mass on unenhanced CT that is heterogeneous could be RCC (23). However, it is very difficult to differentiate small RCCs with homogeneous low density or iso-density compared to the renal parenchyma.

Although most incidental renal masses are benign, most RCCs are identified incidentally (17,24). Therefore, close attention should be paid when diagnosing renal masses as benign cysts on unenhanced CT alone. Incidental detection of small lesions assumed to be RCCs has increased significantly in the past few decades (7). Approximately 13–27% of abdominal imaging studies identify an incidental renal lesion (25). The malignancy risk of renal masses is related to their size and increasing tumor size is associated with a higher possibility of a lesion being malignant rather than benign (26). With increasing detection of RCC at an earlier stage, partial nephrectomy and nephron-sparing surgery have evolved as effective alternatives to radical nephrectomy. Use of partial nephrectomy continues to increase and >65% of patients with tumors ≤4 cm in size have received partial nephrectomies recently (27,28). In such circumstances, it is important to understand how accurate unenhanced CT is for detection of RCC in relation to minimally invasive management. Radiologists are often challenged when diagnosing small renal masses, while it is important to diagnose RCC at an early curable stage. Accordingly, it is also important to be aware of the limits of unenhanced CT for detecting and differentiating small

RCCs. Further efforts will be needed to improve the detectability of T1a RCC on unenhanced CT.

This study had several limitations. First, the sample size was relatively small and tumor pathological types were limited, which could be expected because our patient cohort was obtained from a single institution. We should have discussed the differences of detection and accurate diagnosis between popular clear cell RCC and RCCs such as papillary, chromophobe, and other types. However, the number of RCCs other than clear cell type was small and it was difficult to discuss the matter. We must prospectively examine more patients from multiple institutions in the future. Second, the readers were specifically instructed to search for RCCs on the images and there was variation in the size of benign cysts that might have resulted in improved accuracy. This would significantly skew the bias toward correctly diagnosing RCC because the readers were looking for RCC and the prevalence of RCC versus cysts in this population is much higher than in the general population where this would normally be applied. Third, the present study is the lack of benign renal masses other than cysts. Most RCCs are usually detected as a solid tumor in the renal parenchyma on unenhanced CT in a routine practice. Therefore, oncocytoma and/or acute myeloid leukemia rather than renal simple cysts are preferable as materials. If such benign solid tumors are targeted instead of renal cysts, then diagnostic accuracy may be affected. Fourth, reformats and thinner section reconstructions were not reviewed; this could have improved detectability. Fifth, it is necessary to exclude other influences such as contour type when considring the influence of location in detecting T1a RCC. Last, the only quantitative measurement investigated was size; absolute HU and HU variation were not investigated. There was a suggestion that heterogeneity correlates with the likelihood of malignancy; therefore, this could have been quantitatively investigated.

In conclusion, both tumor size and contour influence the detection and differentiation of T1a RCC on unenhanced CT. It is difficult and dangerous to evaluate the presence or absence of T1a RCC on unenhanced CT alone. Even if it is known in advance that the RCCs exist, the correct diagnosis rate for T1a RCCs remains at 66.4% on unenhanced CT. When examination of the abdominal region is performed, it is important to recognize the limitation of unenhanced CT for detecting T1a RCC. However, thorough knowledge of characteristic findings of small RCC on unenhanced CT and appropriate CT display technics may improve detectability of T1a RCC even on screening unenhanced CT.

## Declaration of conflicting interests

## Funding

## ORCID iD

Aiko Gobara ⓘD https://orcid.org/0000-0002-6031-2810
Takeshi Yoshizako ⓘD https://orcid.org/0000-0003-1623-1375
Rika Yoshida ⓘD https://orcid.org/0000-0002-9157-643X
Megumi Nakamura ⓘD https://orcid.org/0000-0003-2361-2424

## References

1. O'Connor SD, Pickhardt PJ, Kim DH, et al. Incidental finding of renal masses at unenhanced CT: prevalence and analysis of features for guiding management. *Am J Roentgenol* 2011;197:139–145.
2. Dalrymple NC, Verga M, Anderson KR, et al. The value of unenhanced helical computerized tomography in the management of acute flank pain. *J Urol* 1998;159:735–740.
3. Vieweg J, Teh C, Freed K, et al. Unenhanced helical computerized tomography for the evaluation of patients with acute flank pain. *J Urol* 1998;160:679–684.
4. Jewett MA, Zuniga A. Renal tumor natural history: the rationale and role for active surveillance. *Urol Clin North Am* 2008;35:627–634.
5. Kummerlin IP, ten Kate FJ, Wijkstra H, et al. Changes in the stage and surgical management of renal tumours during 1995–2005: an analysis of the Dutch national histopathology registry. *BJU Int* 2008;102:946–951.
6. Sanchez-Martin FM, Millan-Rodriguez F, Urdan-eta-Pignalosa G, et al. Small renal masses: incidental diagnosis, clinical symptoms, and prognostic factors. *Adv Urol* 2008;2008:310694.
7. Gill IS, Aron M, Gervais DA, et al. Clinical practice. Small renal mass. *N Engl J Med* 2010;362:624–634.
8. Duchene DA, Lotan Y, Cadeddu JA, et al. Histopathology of surgically managed renal tumors: analysis of a contemporary series. *Urology* 2003;62:827–830.
9. Patard JJ. Incidental renal tumours. *Curr Opin Urol* 2009;19:454–458.
10. Bosniak MA. The small (≤3.0 cm) renal parenchymal tumor: detection, diagnosis, and controversies. *Radiology* 1991;179:307–317.
11. Remzi M, Ozsoy M, Klingler HC, et al. Are small renal tumors harmless? Analysis of histopathological features according to tumors 4 cm or less in diameter. *J Urol* 2006;176:896–899.
12. Chawla SN, Crispen PL, Hanlon AL, et al. The natural history of observed enhancing renal masses: meta-analysis and review of the world literature. *J Urol* 2006;175:425–431.
13. Brierley JD, Gospodarowicz MK, Wittekind C. *TNM Classification of Malignant Tumours*. 8th ed. Oxford: Wiley Blackwell, 2017.
14. O'Connor SD, Silverman SG, Cochon LR, et al. Renal cancer at unenhanced CT: imaging features, detection rates, and outcomes. *Abdom Radiol (NY)* 2018;43:1756–1763.
15. Pooler BD, Pickhardt PJ, O'Connor SD, et al. Renal cell carcinoma: attenuation values on unenhanced CT. *Am J Roentgenol* 2012;198:1115–1120.
16. Jung SI, Park HS, Kim YJ, et al. Unenhanced CT for the detection of renal cell carcinoma: effect of tumor size and contour type. *Abdom Imaging* 2014;39:348–357.
17. Jayson M, Sanders H. Increased incidence of serendipitously discovered renal cell carcinoma. *Urology* 1998;51:203–205.
18. Schieda N, Vakili M, Dilauro M, et al. Solid renal cell carcinoma measuring water attenuation (-10 to 20 HU) on unenhanced CT. *Am J Roentgenol* 2015;205:1215–1221.
19. Parsons RB, Canter D, Kutikov A, et al. RENAL nephrometry scoring system: the radiologist's perspective. *Am J Roentgenol* 2012;199:W355–359.
20. Kundel HL, Polansky M. Measurement of observer agreement. *Radiology* 2003;228:303–308.
21. Sahi K, Jackson S, Wiebe E, et al. The value of "liverwindows" settings in the detection of small renal cell carcinomas on unenhanced computed tomography. *Can Assoc Radiol J* 2014;65:71–76.
22. Herts BR, Silverman SG, Hindman NM, et al. Management of the incidental renal mass on CT: A white paper of the ACR Incidental Findings Committee. *J Am Coll Radiol* 2018;15:64–273.
23. Silverman SG, Israel GM, Trinh QD. Incompletely characterized incidental renal masses: emerging data support conservative management. *Radiology* 2015;275:28–42.
24. Zhang J, Lefkowitz RA, Bach A. Imaging of kidney cancer. *Radiol Clin North Am* 2007;45:119–147.
25. Hara AK, Johnson CD, MacCarty RL, et al. Incidental extracolonic findings at CT colonography. *Radiology* 2000;215:353–357.
26. Frank I, Blute ML, Cheville JC, et al. Solid renal tumors: an analysis of pathological features related to tumor size. *J Urol* 2003;170:2217–2220.
27. Canter D, Kutikov A, Manley B, et al. Utility of the R.E.N.A.L. nephrometry scoring system in objectifying treatment decision-making of the enhancing renal mass. *Urology* 2011;78:1089–1094.
28. Thompson RH, Kaag M, Vickers A, et al. Contemporary use of partial nephrectomy at a tertiary care center in the United States. *J Urol* 2009;181:993–997.